

# Understanding the propagation of excitations in quantum spin chains with different kind of interactions

Alejandro Ferrón<sup>(1)</sup>, Pablo Serra<sup>(2)</sup> and Omar Osenda<sup>(2)</sup>

(1) *Instituto de Modelado e Innovación Tecnológica (CONICET-UNNE) and Facultad de Ciencias Exactas, Naturales y Agrimensura, Universidad Nacional del Nordeste, Avenida Libertad 5400, W3404AAS Corrientes, Argentina.*

(2) *Instituto de Física Enrique Gaviola, Universidad Nacional de Córdoba, CONICET, Facultad de Matemática, Astronomía, Física y Computación, Av. Medina Allende s/n, Ciudad Universitaria, CP:X5000HUA Córdoba, Argentina*

(Dated: January 3, 2022)

The dynamical behaviour of the quantum state of different quantum spin chains, with designed site dependent interaction strengths, is analyzed when the initial state belongs to the one excitation subspace. It is shown that the inhomogeneous chains are able to transfer excitations with near perfect fidelity. This behaviour is found for two very different spin chain Hamiltonians. The first one is the ferromagnetic Heisenberg Hamiltonian with nearest neighbor interactions, the second one describes a chain with long range anisotropic interactions which are ferromagnetic in the  $z$  direction and antiferromagnetic in the  $(x, y)$  plane. It is shown that both designed chains have in common a partially ordered spectrum and well localized eigenvectors. This physical trait unifies the description of both kind of systems.

PACS numbers:

## I. INTRODUCTION

The dynamical evolution on the one excitation subspace has been studied in a number of context ranging from the propagation of correlations in disordered quantum spin chains [1] to the transfer of quantum states [2–4].

When the Hamiltonian of the spin chain is ferromagnetic the link between the propagation of a single excitation and the transfer fidelity of arbitrary one-spin states is direct [3], since the fidelity of the transfer process can be written rather easily in terms of the probability that an excitation prepared in one extreme of the chain will be transferred to the other extreme.

The availability of numerous physical systems where it is possible to actually implement the transfer protocols [5–15] has driven the study of different control strategies to achieve the propagation of excitations in a ballistic way, *i.e.* the propagation of a spin wave packet that propagates at constant velocity along the chain. Nevertheless, this simple physical behaviour can not be achieved easily in most quantum systems or in the spin chains that model its behaviour.

Much progress has been made using time-dependent control techniques to achieve near perfect quantum state transfer (QST) [16–21], but the conclusions of those studies are, at some extent, particulars and do not inform about general physical traits that lead to the design of general simple pulses that are applicable to different systems. This is not necessarily a bad scenario, most spin chains are controllable [16, 22–24] with a reduced number of control functions (or a reduced number of actuators) and the transmission of information is doable at times that scale linearly or quadratically with the chain length

$N$  [16–20].

More recently there is a renewed interest in the QST problem without any external forcing since the fabrication techniques of microscopic quantum systems allow to build systems with tailored interactions with time-independent but site-dependent variable strength. Modulating the strength of the interaction in order to achieve perfect or near perfect QST with autonomous time evolution instead of a forced evolution has been the subject of many recent works [25–27].

For Heisenberg chains it is known that perfect QST transfer is not achievable even changing the strength of the exchange couplings [28–31]. For more complicate models this is not even know, in many cases the analytical study of the system is too cumbersome to reach any conclusion. Having this in mind, the problem of QST can be cast as an optimization problem, in which the probability that an excitation will be transferred between the extremes of a spin chain is the cost function to be maximized, and the set of possible strength of the interactions the parameter space, where the optimal values of the interactions must be found [32, 33].

Using a Global Optimization method guarantees that some good maximum value will be found [34, 35]. We apply the pivot method to two models, the Heisenberg Hamiltonian and an anisotropic dipolar Hamiltonian, which has been studied as an approximation to the Hamiltonian of cold atoms in optical traps [36–38]. Besides showing that, effectively, the optimization method finds interaction strengths compatible with near perfect QST we show that the optimal strengths have a simple physical interpretation, that unifies the description of the time evolution of the quantum state in long and short range models, irrespective of their isotropic or anisotropic character. Our results also show that the consequent

dynamical evolution is smoother than the observed for homogeneous chains whose time-evolution is marred by dynamical localization effects.

The paper is organized as follows, in Section II the details of the pivot method, and how to apply it to the short and long range models, are presented. In Section III the results obtained for the propagation of excitations optimizing a variable number of parameters that define the spin chains are presented, while the results concerning the general properties of the spectrum and eigenvalues of spin chains that show near perfect quantum state transfer are presented in Section IV. The behaviour of the inverse participation ratio [39, 40] as a dynamical quantity is studied in Section V, in particular the study focuses in the conditions that ensure a smooth, fast and efficient transfer of quantum states. Finally, in Section VI we discuss our results and our conclusions are presented.

## II. MODELS AND METHOD

We will focus our study in two well-known quantum spin chain Hamiltonians, the isotropic short-range Heisenberg Hamiltonian

$$H_{short} = - \sum_{i=1}^{N-1} J_i (\sigma_i^x \sigma_{i+1}^x + \sigma_i^y \sigma_{i+1}^y + \sigma_i^z \sigma_{i+1}^z), \quad (1)$$

where  $J_i > 0$ , and the anisotropic long-range dipolar Hamiltonian

$$H_{long} = \sum_{i < j}^N \frac{J}{|x_i - x_j|^3} (c_x \sigma_i^x \sigma_j^x + c_y \sigma_i^y \sigma_j^y + c_z \sigma_i^z \sigma_j^z), \quad (2)$$

where  $J > 0$ ,  $c_x = c_y = 1$  and  $c_z = -2$ , *i.e.* the distance dependent exchange couplings in the plane are antiferromagnetic while in the  $z$  direction the exchange couplings are ferromagnetic. This last Hamiltonian can be found as the weak limit of the Hamiltonian of a chain of cold atoms. In the following we will call a particular set of  $N - 1$  exchanges coefficients  $J_i$  an Exchange Coefficients Distribution (ECD). In what follows we always consider *centro-symmetric* chains, *i.e.*  $J_i = J_{N-i}$ , while for the long range model  $|x_i - x_j| = |x_{N-i+1} - x_{N-j+1}|$ .

The transfer properties of both Hamiltonians have been studied extensively when the chains are homogeneous, *i.e.* all the  $J_i$  coefficients in Eq. (1) are equal,  $J_i = J_h, \forall i$ , and  $|x_i - x_{i+1}| = d > 0, \forall i$  in Eq. (2). In particular, for the Heisenberg Hamiltonian it is known that the homogeneous chain is quite poor as a transfer channel when the simplest transfer protocol is implemented.

Both Hamiltonians commute with the total magnetization in the  $z$ -direction

$$\left[ H, \sum_i \sigma_i^z \right] = 0, \quad (3)$$

so both Hamiltonians can be diagonalized in subspaces with fixed number of excitations, *i.e.* in subspaces with a given number of spins up. It is customary to use the computational basis, where for a single spin  $|0\rangle = |\downarrow\rangle$  and  $|1\rangle = |\uparrow\rangle$ , so  $|\mathbf{0}\rangle = |000\dots 0\rangle$  is the state with zero spins up of the whole chain, and

$$\sum_{i=1}^N \sigma_i^z |\mathbf{0}\rangle = -N |\mathbf{0}\rangle. \quad (4)$$

The  $N$  states with a single spin up are denoted as follows

$$|\mathbf{1}\rangle = |10\dots 0\rangle, |\mathbf{2}\rangle = |010\dots 0\rangle, \dots, |\mathbf{N}\rangle = |00\dots 1\rangle. \quad (5)$$

*i.e.* the state  $|\mathbf{j}\rangle$  is the state of the chain with only the  $j$ -th spin up. The one-excitation basis plays a fundamental role in the simplest transfer protocol. In this protocol the initial state of the chain,  $|\Psi(0)\rangle$ , is prepared as

$$|\Psi(0)\rangle = |\psi(0)\rangle \otimes |\mathbf{0}\rangle_{N-1}, \quad (6)$$

where  $|\psi(0)\rangle = \alpha|0\rangle + \beta|1\rangle$ , is an arbitrary one-spin pure state, with  $\alpha$  and  $\beta$  complex constants such that  $|\alpha|^2 + |\beta|^2 = 1$ , and  $|\mathbf{0}\rangle_{N-1}$  is the state without excitations of a chain with  $N - 1$  spins. The state in Eq. (6) can be rewritten as

$$|\Psi(0)\rangle = \alpha|\mathbf{0}\rangle + \beta|\mathbf{1}\rangle. \quad (7)$$

Using the time evolution operator

$$U(t) = \exp(-iHt), \quad (8)$$

the state of the chain at time  $t$  can be obtained as

$$|\Psi(t)\rangle = U(t)|\Psi(0)\rangle = \alpha U(t)|\mathbf{0}\rangle + \beta U(t)|\mathbf{1}\rangle. \quad (9)$$

It is clear that the state transfer is perfect when for some time  $T_{per}$  the state of the chain is given by

$$|\Psi(T_{per})\rangle = e^{i\theta} (\alpha|\mathbf{0}\rangle + \beta|\mathbf{N}\rangle), \quad (10)$$

where  $\theta$  is some real arbitrary phase. So, the transfer fidelity as a function of time is calculated as

$$f_{\alpha,\beta}(t) = |\alpha\langle\Psi(t)|\mathbf{0}\rangle + \beta\langle\Psi(t)|\mathbf{N}\rangle|^2. \quad (11)$$

The fidelity in Eq. (11) depends on the particular initial state, Eq. (7), chosen to be transferred. Usually, to quantify the quality of the state transfer protocol, it is introduced the average of  $f_{\alpha,\beta}(t)$  over all the possible values of  $\alpha$  and  $\beta$ . It can be shown that this averaged fidelity,  $F(t)$ , can be written as

$$F(t) = \frac{\sqrt{|P(t)|}}{3} + \frac{P(t)}{6} + \frac{1}{2}, \quad (12)$$

where

$$P(t) = |\langle \mathbf{1} | U(t) | \mathbf{N} \rangle|^2 \quad (13)$$

is called the transferred population between the first and last sites of the chain, and we assume that  $\cos(\gamma) = 1$ , where  $\gamma = \arg(f_{\alpha,\beta}(t))$ , as in Ref. [2]. The pretty good transfer occurs when for some  $t_\epsilon$

$$P(t_\epsilon) = 1 - \epsilon, \quad \forall \epsilon > 0. \quad (14)$$

The idea behind our method is quite simple and can be stated as follows: it is simpler to use inhomogeneous chains with site-dependent exchange coefficients tailored to achieve a high probability of transfer which is carried out by the autonomous dynamics of the system than to control the dynamics using time-dependent pulses. The tailoring is made using a Global optimization method that finds a good maximum value for  $P(T)$  irrespective of the Hamiltonian or the arrival time  $T$ .



FIG. 1: The cartoon depicts how the pivot method works. Starting from  $K$  randomly chosen probes (the cross-like red dots) the cost function is evaluated for each one of them. Then, the  $K/2$  probes with the largest values of the cost function are kept (those with the lowest values are discarded) and the method *pivots* over them to generate other  $K/2$  new ones. The cost function is evaluated and the convergence checked. If the convergence criterion is not satisfied new rounds of discarding and pivoting are repeated until convergence is achieved.

In Reference [32] we used a Global optimization method to obtain chains that showed near perfect QST so the detailed description of the method can be consulted there. Here we describe briefly how the method proceeds for the short range model, but the procedure is exactly the same for any one-dimensional chain.

The search for an optimal value of a given cost function, that depends on a number of variables, starts from a set of probes which are randomly generated in a hypercube whose side length is chosen to contain the possible values of the variables that determine the value of the

cost function. In the cartoon in Figure 1 the yellow rectangle depicts the hypercube and the starry dots show the set of probes. For the initial set of  $K$  probes the cost function is evaluated and the set of  $K/2$  probes with the larger values of the cost function are kept. Then the pivot method generates new  $K/2$  probes. After this step convergence is checked and if the criterion is satisfied the probe with the largest cost function value is selected. If the convergence is not achieved  $K/2$  probes are discarded (those with the lower values of the cost functions) and the pivot method is called again (for more details see References [34, 35]). This steps are depicted in the cartoon, the green arrows showing the direction that the algorithm takes until the convergence is achieved.

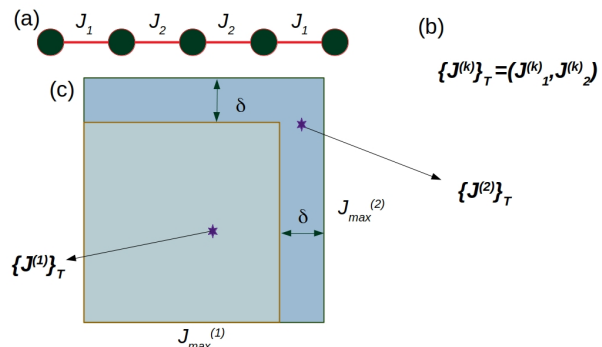


FIG. 2: The cartoon depicts the ingredients of the procedure designed to find ECD's that can be used to achieve near perfect QST. a) A centro-symmetric spin chain with five spins and only two different exchange couplings  $J_1$  and  $J_2$ . b) For the five spin chain a ECD that optimize the cost function for an arrival time  $T$  is obtained using the pivot method. The ECD is denoted by  $\{J^{(k)}\}_T = (J_1^{(k)}, J_2^{(k)})$ , which is a point in the hypercube with side length  $J_{max}^{(k)}$ . c) The smaller hypercube with side length  $J_{max}^{(1)}$  and the second one smaller, with side length  $J_{max}^{(2)} = J_{max}^{(1)} + \delta$ , are depicted using light blue and blue squares. The corresponding ECD that optimize the cost function for each hypercube is depicted as a starry dot inside the hypercube.

It is clear that for problems of QST the cost function to be maximized is the PT,  $P(T)$ , at some arrival time,  $t = T$ . For general problems the side length of the hypercube should be carefully chosen, since the volume of the hypercube is  $L^M$ , where  $M$  is the number of variables that determine the value of the cost function. Because of this we proceed as follows, first we start using the pivot method in a hypercube with a relatively small side length and applying the pivot method a first ECD is determined,  $\{J^{(1)}\}_T$ , which maximizes the PT for an arrival time  $T$ . Then the side length of the hypercube is increased and a second ECD is obtained,  $\{J^{(2)}\}_T$ . This procedure is depicted in the cartoon in Figure 2 for a centro-symmetric chain with five spins that has only two different exchange couplings. The initial hypercube is depicted with light blue square with side length  $J_{max}^{(1)}$  while the second hypercube with side length  $J_{max}^{(2)}$  is depicted

as a darker blue square. The notation is used to emphasize the succession of values obtained. Calling  $P^{(k)}(T)$  to the PT value obtained using the ECD  $J_{max}^{(k)}$ , it is fulfilled that

$$P^{(1)}(T) \leq P^{(2)}(T) \leq P^{(3)}(T) \leq \dots \quad (15)$$

In [32] it is shown that for anisotropic and isotropic Heisenberg Hamiltonians with only nearest neighbors interactions the side length of the successive hypercubes is a decreasing function of the arrival time and is bounded above by  $N$ .

It is worth to point out that for  $k$  large enough the optimization method converges to a given “optimal” ECD and PT, this value for the PT is the one that is plotted in the figures of the next Sections. Nevertheless, sometimes it is useful to study the behaviour of the ECD for smaller values of the PT to understand how the spectral properties of a given Hamiltonian change with the value of the target PT.

The procedure described above can be easily translated to other Hamiltonians. For the long range dipolar Hamiltonian in Eq. (2) we consider the distances between nearest neighbors  $\{|x_i - x_{i+1}|\}_{i=1}^{N-1}$  as the variables to be explored by the pivot method. The cost function is again the PT at some arrival time  $T$ .

### III. QST OPTIMIZING A VARIABLE NUMBER OF EXCHANGE COEFFICIENTS

In Reference [32] it was shown that the optimization procedure produces ECDs  $\{J^{(k)}\}_T$ , for  $k$  large enough, that result in near perfect QST when the Hamiltonian of the chain is of the  $XXZ$  type with nearest neighbors interactions. In this Section we want to address two related questions. The first one is: if only a few exchange coefficients (or distances) can be optimized, due to some implementation limitation, is it possible to achieve near perfect or very good QST? The second one is: short range and long range spin chains with only few quantities optimized behave in a similar way?

Figure 3 summarizes our results about the two questions stated above. The figure shows the population transferred, for different chain lengths and optimizing (from bottom to top) one, two, three or  $N/2$  exchange couplings or distances, accordingly with the model. The arrival time considered is  $T = 2N$ . The left panel shows the results found for the Heisenberg model, while the right one shows the results found for the anisotropic long-range dipolar model. It is clear that the PT is an increasing function of the number of exchange couplings optimized, which is to be expected. Nevertheless, what is striking is the fact that the long range model increases its efficiency as a quantum channel faster than the short range one. Of course, if the  $N/2$  exchange couplings or distances are optimized the GO method provides chains

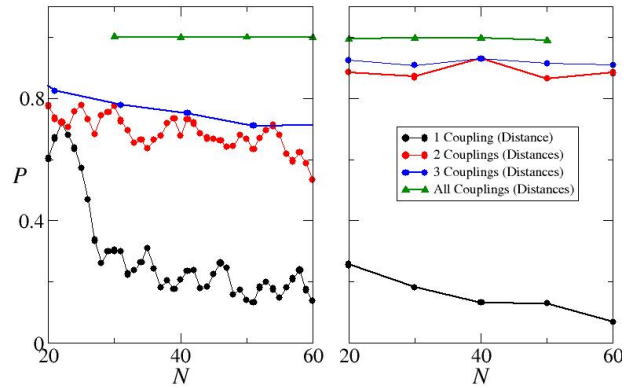


FIG. 3: The population transferred as a function of the chain length  $N$ . Panel a) shows the results obtained for the short range model, panel b) shows the results for the long range model. From bottom to top the curves are obtained optimizing one (black dots and curve), two (red), three (blue) and all (green) the exchange couplings coefficients.

that show near perfect QST. Similar scenarios can be found for other arrival times.

The results shown in Figure 3, despite its usefulness, do not provide an insight about the physical mechanisms that is responsible of the increased efficiency of the chains with more exchange couplings optimized. The next Sections are devoted to understand these mechanisms.

### IV. EIGENVECTOR LOCALIZATION AND PARTIALLY ORDERED SPECTRUM

Following Kay [28], near perfect QST can be expected in Heisenberg spin chains whose spectrum satisfies  $E_{i+1} - E_i \sim q_i \alpha$ , where  $q_i$  is an odd natural number, *i.e.* successive energy values should differ in odd multiples of a constant  $\alpha$ , approximately.

Figure 4a) shows the difference between successive eigenvalues,  $\Delta_i = E_{i+1} - E_i$  for a chain with  $N = 20$  spins *vs* the eigenvalue index  $i$ , for chains with different number of distances optimized. The arrival time considered is  $T = 2N = 40$ . The distance  $\Delta_i$  is scaled with  $\pi/T$ . It is clear that the number of eigenvalues that satisfies  $\Delta_i/(\pi/T) \sim q_i$ , increases as a function of the number of distances optimized. The inset shows that  $\Delta_i/(\pi/T) \sim 1$  is satisfied with a remarkable precision when  $N/2$  distances are optimized. We called this scenario a partially ordered spectrum.

The time dependent state of the chain can be written as

$$\psi(t) = \sum_{\tilde{i}} \chi_{\tilde{i}} \exp(-iE_{\tilde{i}}t) + \sum_{i \neq \tilde{i}} \chi_i \exp(-iE_i t), \quad (16)$$

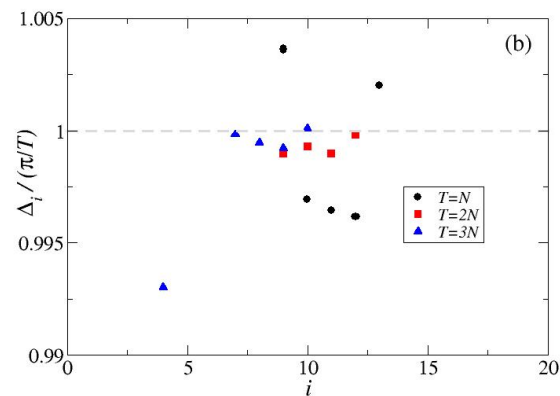
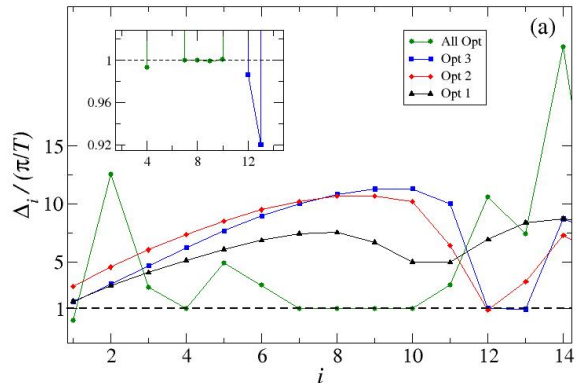


FIG. 4: The scales difference between successive eigenvalues,  $\Delta_i$ , for the optimal exchange coupling distribution *vs* the index  $i$ , for a chain with length  $N = 20$  and an arrival time  $T = 2N$ . a) As in Figure 3, the data corresponding to the results obtained optimizing one, two, three or all the exchange couplings are shown using black, red, blue and green dots, respectively. Panel b) shows a detailed view of the zone near  $\Delta_i = 1$ , for a chain with length  $N = 40$  spins and different arrival times.

where the index  $\tilde{i}$  runs over the eigenvalues that satisfies  $\Delta_{\tilde{i}}/(\pi/T) \sim q_i$ , then at  $t = T$  the terms on the first sum will interfere constructively. Near perfect QST occurs at arrival time  $T$  when a number of terms in Eq. (16) interfere constructively to produce  $|\langle \psi(T) | N \rangle|^2 \sim 1$ . The relatively reduced number of eigenvalues that satisfies approximately the constructive interference condition

$$\Delta_i/(\pi/T) = q_i \quad (17)$$

indicates that to obtain near perfect QST it is necessary to get  $\chi_i \sim 0$  for  $i \neq \tilde{i}$ . Note that, as is shown in Figure 4b), the number of eigenvalues that approximately satisfies the constructive interference condition does not change very much when the arrival time is increased, but those near unity become even closer to it.

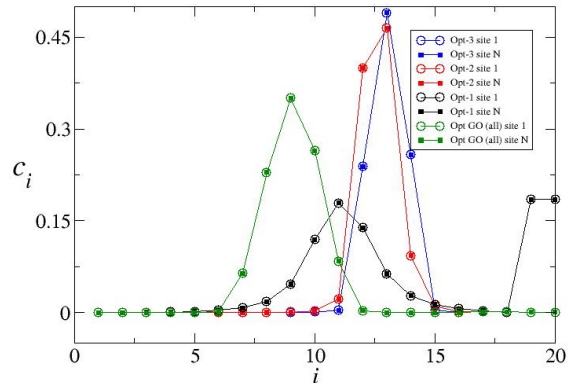


FIG. 5: The figure shows the coefficients  $c_i = |\langle v_i | \mathbf{1} \rangle|^2$ , the square modulus of the scalar product between the  $i$ -th eigenvector,  $|v_i\rangle$ , and  $|\mathbf{1}\rangle$ , *vs*  $i$ . Again, the results corresponding to the optimization of one, two, three or all the exchange couplings are shown using black, red, blue and green dots, respectively.

Figure 5 shows the coefficients  $c_i = |\langle v_i | \mathbf{1} \rangle|^2$  *vs*  $i$ , where the vectors  $|v_i\rangle$  are solutions of

$$H(J_T)|v_i\rangle = E_i|v_i\rangle. \quad (18)$$

Extended eigenstates have  $c_i \sim 1/N$ , where  $N$  is the chain length. Figure 5 shows that the eigenvectors corresponding to the almost ordered eigenvalues are strongly localized at both extremes of the quantum chain.

In a few words, almost near perfect QST is achievable with a reduced number of eigenvalues satisfying condition (17) as long as their eigenvectors are well localized at the extremes of the spin chain. This scenario was at some extent, envisioned as a necessary condition by Kay and others [28, 30] a requisite to achieve the so called pretty good quantum state transfer, but for the isotropic Heisenberg model. What our results indicate is that the pivot method finds precisely the ECD that result in the almost ordered spectrum with well localized eigenvectors that are required for the almost perfect QST to happen also for the long range model in Eq. (2).

The partially ordered spectrum with well localized eigenvectors scenario is also present in the short range Heisenberg model, Eq. (1) so near perfect QST is also achievable. Nevertheless there are some differences that are worth of further analysis.

Figure 6 shows a)  $\Delta_i$  and b)  $c_i$  both *vs* the index  $i$  for the Heisenberg Hamiltonian and a chain with  $N = 60$  spins. There is a large number of successive eigenvalues that satisfy the condition in Eq. (4), anyway those that satisfy the condition with  $q_i = 1$  are a minority. In the figure, values of  $\Delta_i = 15, 17$  can be clearly appreciated. The appearance of values of  $\Delta_i$  is related to the different propagation velocities that are characteristic of the Heisenberg model. Nevertheless, Figure 6 b) shows again,



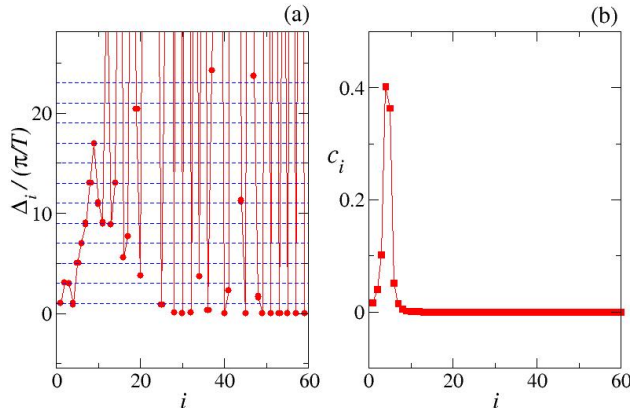


FIG. 6: The scaled difference between successive eigenvalues,  $\Delta_i$ , and the  $c_i$  coefficients, are shown in panels a) and b), respectively, both *vs* the index  $i$  for a chain with a short range Heisenberg Hamiltonian. The chain has  $N = 60$  spins. In panel a) the partially ordered spectrum can be clearly appreciated at the edge of the eigenvalues band, with values of  $\Delta_i$  close to odd naturals as large as 15 or 17. The data in panel b) shows that only the eigenvectors corresponding to the partially ordered portion of the spectrum are localized at the extremes of the chain.

that the eigenvectors associated to the part of the spectrum that is partially ordered are well localised at the extremes of the chain. Other feature that distinguishes the spectra of the short and long range model is that in the spectrum of the former there is a number of very small eigenvalues,  $E_i \sim 0$ .

Since the optimization method is interrupted when the criterion of convergence is fulfilled it is natural to wonder about the spectrum of Hamiltonians that correspond to ECD obtained with sub-optimal convergence criteria, *i.e.* when the PT is far from near perfect QST.

Figure 7 a) shows the distance  $d_i$  which is defined as the difference between  $\Delta_i$  and its nearest odd natural for four different values of the PT. The values were obtained allowing the optimization of all the couplings. The data in the figure shows that the number of ordered pair of eigenvalues is an increasing function of the transferred probability at a given arrival time. Even for the largest PT achieved, that differs from the unity in less than  $2 \times 10^{-4}$ , only a third of the eigenvalues are very close to an odd natural number, emphasizing that the localization of the corresponding eigenvectors is also required to achieve near perfect QST. The behaviour of the coefficient that measures how localized are the eigenvectors at the extremes of the chain can be observed in Figure 7 b).

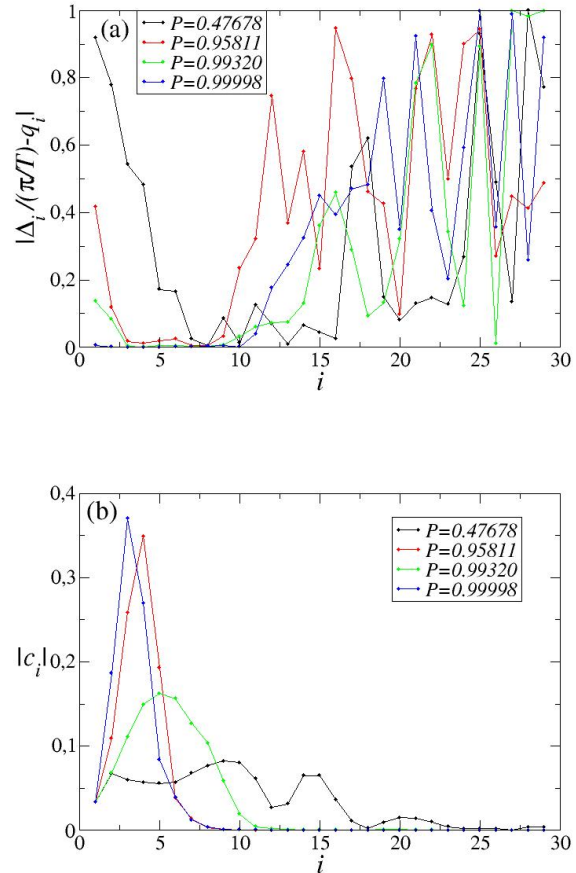


FIG. 7: The scaled difference between successive eigenvalues,  $\Delta_i$  minus the closest odd integer,  $q_i$ , and the  $c_i$  coefficients, are shown in panels a) and b), respectively, both *vs* the index  $i$  for a chain with a short range Heisenberg Hamiltonian. The chain has  $N = 30$  spins, arrival time  $T = N$  and the data is obtained interrupting the optimization procedure at sub-optimal PT (see the text for more details). The panels show the values obtained for PT values of 0.9998, 0.99320, 0.95811 and 0.47678 using blue, red, green and black dots, respectively. The lines are included as a guide to the eye. Panel a) shows how the partially ordered portion of the spectrum increases when the PT value becomes larger. The localization of the corresponding eigenvectors is shown in panel b) and it can be appreciated how it becomes stronger for larger values of the PT.

## V. PREVENTING DYNAMICAL LOCALIZATION

Besides the effect of the optimization of the exchange couplings over the spectrum and eigenvectors, which results in very large values for the PT, there are other dynamical effects that take place during the transmission. A quantity that allows to qualitatively understand the changes in the dynamical behaviour of the chain state is the inverse participation ratio (IPR)

$$L(t) = \frac{1}{\sum_i |\chi_i(t)|^4}. \quad (19)$$

The IPR has been used to analyze the dynamical behaviour of many different systems, ordered, chaotic or disordered, since it is able to detect how an initially localized state spreads, or not, over the whole system. The dynamical evolution of an one excitation propagating on Heisenberg-like chains are characterized by rapid fluctuations in the value of the IPR since the dynamics reflects the peculiar distribution of eigenvalues on the spectrum. But, as was shown in Section III the optimization procedure results in chains with partially ordered spectrum so the behaviour of the IPR should reflect the emerging ordering and the appearance of well localized eigenvectors.

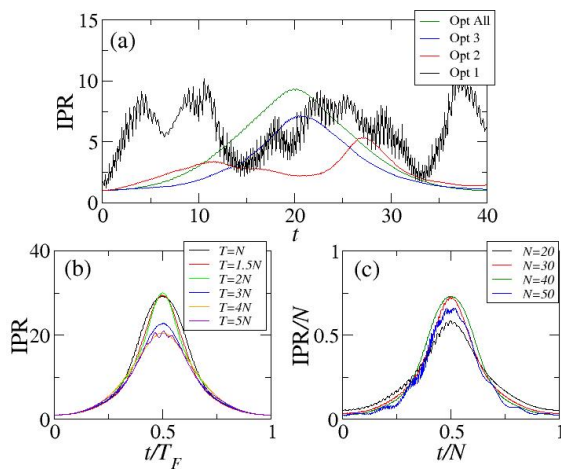


FIG. 8: The IPR as a function of time. Panel a) shows the results calculated when one, two, three or all the exchange coefficients are optimized as black, red, blue and green curves, respectively. The results correspond to a chain with  $N = 20$ , arrival time of  $T = 40$ . The chain considered is described by the long range Hamiltonian. Panel b) shows the behaviour of the IPR for a chain with  $N = 40$  spins but for different arrival times, each curve is plotted *vs* the scaled time  $t/T$ . Panel c) shows the IPR *vs* the scaled time  $t/N$  for chains of different length but with their Hamiltonians optimized for the same arrival time  $T = 40$ .

Figure 8a) shows the time evolution of the IPR, calculated for a chain of  $N = 20$  spins that has the long range dipolar Hamiltonian. The curves are obtained optimizing different number of distances. The effect of the optimization and the progressive building of the partially ordered spectrum is easily appreciated, since the IPR goes from a fast changing functions with rapid oscillations to a smooth function when the number of quantities optimized is increased.

On the other hand, Figure 8 b) and c) show that in the “optimized regime” the dynamical evolution of the excitation propagating in the chain is pretty much the same. Panel b) compares the time evolution of the IPR for a

chain with  $N = 40$  spins and different arrival times, while panel c) shows the same quantity for chains of different length and the same arrival time.

A similar analysis can be carried out with respect to the Heisenberg Hamiltonian. The conclusions are quite similar, and they can be found in Appendix , together with a figure showing the behaviour of the IPR for this case.

## VI. DISCUSSION AND CONCLUSIONS

The role played by localized states in QST settings is well known in the context of XX Hamiltonians, where the regimes known as *border controlled QST* [25] and *optimal dynamics* [26] exploit that changing the values of just one or two exchange couplings at the extremes of centro-symmetric chains results in regimes where near perfect or very good QST is achievable in otherwise homogeneous chains. More recently, Palaiodimopoulos *et al* showed that the localized eigenstates lying at the centre of the eigenvalues band are crucial to obtain fast and robust QST in a topological chain [41], although their protocol involved precise time-dependent control of the exchange couplings at the extremes of a SSH chain,  $J_1(t)$  and  $J_{N-1}(t)$ . As our results show, looking for localized eigenstates located at any region of the spectrum seems to be a requisite to attain near perfect QST in arbitrary spin chains, as long as these eigenstates correspond to the partially ordered portion of the spectrum. Of course, the intricacies of the Bethe ansatz prevents that this traits can be singled out in the Heisenberg Hamiltonian. The perspectives are even worse when the anisotropic long range dipolar Hamiltonian is considered.

As our results suggest, it is harder to find the regime of smooth propagation for the Heisenberg Hamiltonian than for the long range Hamiltonian. This is another manifestation of the “disorderly” way in which the excitations propagate in Heisenberg chains.

It is striking the reduced number of eigenvalues fulfilling Eq. (17) that are really necessary to achieve near perfect QST, as long as their eigenvectors are well localized at the extremes of the chain. Since most studies showing the existence of the pretty good QST focus in the requirements that the eigenvalues should satisfy, it is worth to think if a change of strategy adding this fact could lead to new advances on the design of Hamiltonians that can be implemented in experimental settings.

With respect to the last point commented in the paragraph above, there are at least two possible lines of work. The first one is to extend the ideas in Reference [42], where A. Kay discusses how to obtain near perfect QST in chains with interactions beyond nearest neighbors. The second one requires the implementation of algorithms characteristic of inverse eigenvalue problems, that allow to construct a matrix with prescribed eigenpairs. Work along this lines is in progress

*Acknowledgments* The authors acknowledge partial fi-

nancial support from CONICET (PIP11220150100327, PUE22920170100089CO). O.O and P.S. acknowledges partial financial support from CONICET and SECYT-UNC. A.F. thanks the hospitality of the FAMAF, where a large part of this manuscript was discussed and planned.

### Appendix: IPR behaviour for Heisenberg chains

As has been said in the main text, the behaviour of the IPR as a function of time for Heisenberg chain is similar to the observed in the long range model studied. Anyway, there are some qualitative differences that are interesting to look at. Figure 9 shows the behaviour of the inverse participation ratio, as a function of the time  $t$ , calculated using sub-optimal ECD. The chain considered has  $N = 30$  spins and the optimal ECD corresponds to an arrival time  $T = N$ . Note that, even for values as large as  $P = 0.99$  the IPR shows rapid oscillations. Moreover, the dynamical regimes at both sides of  $P = 0.99$  seem quite different, resulting in a dynamical evolution with a single or double maximum for  $P < 0.99$  and  $P > 0.99$ , respectively. For smaller values of  $P$  the “bell-shape” becomes increasingly distorted until quite rapid oscillations

spoil completely the transfer process (not shown).

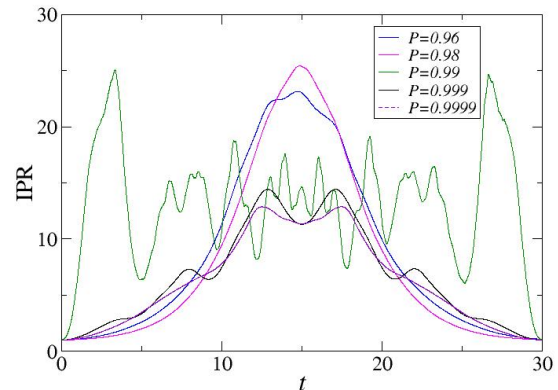


FIG. 9: The behaviour of the inverse participation ratio, as a function of the time  $t$ , calculated using sub-optimal ECD. The chain considered has  $N = 30$  spins and the optimal ECD corresponds to an arrival time  $T = N$ .

- 
- [1] C. K. Burrell and T. J. Osborne, Phys. Rev. Lett. **99**, 167201 (2007).
- [2] S. Bose, Phys. Rev. Lett. **91**, 207901 (2003).
- [3] S. Bose, Contemporary Physics, 48:1, 13-30 (2007)
- [4] G.M. Nikolopoulos and I. Jex (Edts.), *Quantum State Transfer and Network Engineering*, Springer-Verlag Berlin Heidelberg 2014
- [5] Y. P. Kandel, H. Qiao, and J. M. Nichol, Appl. Phys. Lett. **119**, 030501 (2021).
- [6] F. Martins, F. K. Malinowski, P. D. Nissen, S. Fallahi, G. C. Gardner, M. J. Manfra, C. M. Marcus, and F. Kuemmeth, Phys. Rev. Lett. **119** 227701 (2017).
- [7] V. Kostak, G. M. Nikolopoulos, and I. Jex, Phys. Rev. A **75**, 042319 (2007)
- [8] D. M. Zajac, T. M. Hazard, X. Mi, E. Nielsen, and J. R. Petta, Phys. Rev. Applied **6**, 054013 (2016).
- [9] X. Li, Y. Ma, J. Han, Tao Chen, Y. Xu, W. Cai, H. Wang, Y.P. Song, Zheng-Yuan Xue, Zhang-qi Yin, and Luyan Sun, Phys. Rev. Applied **10**, 054009 (2018)
- [10] Jingfu Zhang, Gui Lu Long, Wei Zhang, Zhiwei Deng, Wenzhang Liu, and Zhiheng Lu, Phys. Rev. A **72**, 012331 (2005); P. Cappellaro, C. Ramanathan, and D. G. Cory, Phys. Rev. A **76**, 032317 (2007); J. Zhang, M. Ditty, D. Burgarth, C. A. Ryan, C. M. Chandrashekar, M. Laforest, O. Moussa, J. Baugh, and R. Laflamme, Phys. Rev. A **80**, 012316 (2009)
- [11] N. J. S. Loft et al New J. Phys. **18** 045011 (2016).
- [12] L. Banchi, A. Bayat, P. Verrucchi, and S. Bose, Phys. Rev. Lett. **106**, 140501 (2011).
- [13] R. J. Chapman, M. Santandrea, Zixin Huang, G. Corrielli, A. Crespi, Man-Hong Yung, R. Osellame and A. Peruzzo, Nat. Comm. **7**, 11339 (2016).
- [14] Y. P. Kandel, H. Qiao, S. Fallahi, G. C. Gardner, M. J. Manfra, J. M. Nichol, Nature **573**, 553 (2019).
- [15] E. Baum, A. Broman, T. Clarke, N. C. Costa, J. Mucciaccio, A. Yue, Yuxi Zhang, V. Norman, J. Patton, M. Radulaski, and R. T. Scalettar, arXiv:2112.05740
- [16] X. Wang, D. Burgarth, and S. Schirmer, Phys. Rev. A **94**, 052319 (2016).
- [17] D. Burgarth, K. Maruyama, M. Murphy, S. Montangero, T. Calarco, F. Nori, and M. Plenio, Phys. Rev. A **81**, 040303(R) (2010).
- [18] S. Yang, A. Bayat, S. Bose, Phys. Rev. A **82**, 022336 (2010) .
- [19] X.P. Zhang, B. Shao, S. Hu, J. Zou, L.A. Wu, Ann. Phys. **375** (2016) 435–443.
- [20] U. Farooq, A. Bayat, S. Mancini, S. Bose, Phys. Rev. B **91**, 134303 (2015).
- [21] D. S. Acosta Coden, S. S. Gómez, A. Ferrón, O. Osenda, Physics Letters A **387** 127009 (2021).
- [22] V. Jurdjevic and H. J. Sussmann, J. Diff. Eqn. **12**, 313 (1972).
- [23] D. Burgarth, S. Bose, C. Bruder, and V. Giovannetti, Phys. Rev. A **79**, 060305(R) (2009).
- [24] V. Ramakrishna, M. V. Salapaka, M. Dahleh, H. Rabitz, and A. Peirce, Phys. Rev. A **51**, 960 (1995).
- [25] A. Zwick, G. A. Álvarez, J. Stolze and O. Osenda, Quantum Information and Computation **15**, 0582 (2015).
- [26] L. Banchi, T. J. G. Apollaro, A. Cuccoli, R. Vaia, and P. Verrucchi, Phys. Rev. A **82**, 052321 (2010).
- [27] L. Banchi, T. J. G. Apollaro, A. Cuccoli, R. Vaia and P. Verrucchi, New J. Phys. **13**, 123006 (2011).
- [28] A. Kay - arxiv-1906.06223
- [29] A. Kay, Int. J. Quantum Inf. **8**,641 (2010).
- [30] L. Banchi, G. Coutinho, C. Godsil, and S. Severini, J. Math. Phys. **58**, 032202 (2017) ,



- [31] C. M. van Bommel, arXiv:2010.06779v1
- [32] P. Serra, A. Ferrón and O. Osenda, arxiv
- [33] Xiao-Ming Zhang, Zi-Wei Cui, Xin Wang, and Man-Hong Yung, Phys. Rev. A **97**, 052333 (2018).
- [34] P. Serra, A. F. Stanton and S. Kais, Phys. Rev. E **55**, 1162 (1997).
- [35] P. Serra, A. F. Stanton, S. Kais and R. E. Bleil, J. Chem. Phys. **106**, 7170 (1997).
- [36] P. Hauke, F. M. Cucchietti , A. Müller-Hermes, M.-C. Bañuls, J. I. Cirac and M. Lewenstein , New Journal of Physics **12**, 113037 (2010)
- [37] D. Porras and J. I. Cirac, Phys. Rev. Lett. **92**, 207901 (2004)
- [38] C.-L.Hung, A. González-Tudela, , J. I. Cirac, and H. J. Kimble, PNAS **113**, 4946 (2016)
- [39] O. Giraud, J. Martin and B. Georgeot, Phys. Rev. A **76**, 042333 (2007).
- [40] A. Zwick and O. Osenda, J. Phys. A: Math. Theor. **44**, 105302 (2011).
- [41] N. E. Palaiodimopoulos, I. Brouzos, F. K. Diakonou, and G. Theocharis, Phys. Rev. A **103**, 052409 (2021).
- [42] A. Kay, Phys. Rev A **73**, 032306 (2006).